Inorg. Chem. **2001,** *40,* 6383−6389

Cd(II) and Pb(II) Complexation by Dipyridine-Containing Macrocycles with Different Molecular Architecture. Effect of Complex Protonation on Metal Coordination Environment

Paloma Arranz,[†] Carla Bazzicalupi,[‡] Andrea Bencini,*[,‡] Antonio Bianchi,*[,‡] Samuele Ciattini,[‡] Patrizia Fornasari,[‡] Claudia Giorgi,[‡] and Barbara Valtancoli[‡]

Department of Inorganic and Organic Chemistry, University of Jaen, Jaen, Spain, and Department of Chemistry, University of Florence, Via della Lastruccia 3, 50019 Sesto Fiorentino, Firenze, Italy

Received June 6, 2001

The coordination features of the three dipyridine-containing polyamine macrocycles 2,5,8,11,14-pentaaza[15]-[15](2,2′)[1,15]-bipyridylophane (**L1**), 5,8,11-trimethyl-2,5,8,11,14-pentaaza[15]-[15](2,2′)[1,15]-bipyridylophane (**L2**), and 4,4′-(2,5,8,11,14-pentaaza[15]-[15](2,2′)-bipyridylophane) (**L3**) toward Cd(II) and Pb(II) have been studied by means of potentiometric, microcalorimetric, and spectrophotometric UV−vis titrations in aqueous solutions. All ligands form 1:1 metal complexes. In the **L1** and **L2** complexes the metals are lodged inside the macrocyclic cavity, coordinated to the heteroaromatic nitrogens. On the other hand, the insertion of a rather rigid dipyridine moiety within a macrocyclic structure does not allow all the aliphatic amine groups to coordinate to the metals and several protonated complexes are found in solution. The particular molecular architecture of **L3**, which displays two well-separated binding moieties, strongly affects its coordination behavior. In the $[\mathrm{Pb}\mathbf{L3}]^{2+}$ complex and in its protonated species, the metal is lodged inside the macrocyclic cavity, not bound to the heteroaromatic nitrogens. A similar coordination environment is found in $[\mathrm{Cd}\mathbf{L3}]^{2+}$. In this case, however, protonation of the complex takes place on the aliphatic amine groups and gives rise to translocation of the metal outside the cavity, coordinated by the dipyridine moiety.

Macrocyclic ligands may contain central hydrophilic cavities ringed with electronegative binding atoms and exterior frameworks exhibiting hydrophobic behavior.[1−15] The hydrophobic exteriors may allow them to solubilize metal ions in nonaqueous solvent or in membrane media, resulting in their employment as models for carrier molecules in the study of active ion transport phenomena as well as in their potential use as sequestering agents for metals of environmental importance, such as Pb(II) or Cd(II). The coordination features of several saturated polyamine macrocycles have been investigated in order to design selective binding agents for these metals.[16−26]

Earlier we reported the synthesis of a series of macrocyclic polyamine ligands containing a dipyridine unit, namely, **L1**−**L3**.[27,28] This heteroaromatic moiety can provide a further binding site for metal cations. This unit is rather rigid and provides two

---

* Authors to whom correspondence should be addressed. E-mail: andrea.bencini@unifi.it.

[†] University of Jaen.

[‡] University of Florence.

(1) Hughes, M. N., *The Inorganic Chemistry of the Biological Processes*; Wiley: New York, 1981.
(2) Bradshaw, J. S., *Aza-crown Macrocycles*; Wiley: New York, 1993.
(3) Izatt, R. M.; Bradshaw, J. S.; Nielsen, S. A.; Lamb, J. D.; Christensen, J. J.; Sen, D. *Chem. Rev.* **1985**, *85*, 271.
(4) Izatt, R. M.; Pawlak, K.; Bradshaw, J. S. *Chem. Rev.* **1991**, *91*, 1721.
(5) Gerasimchuk, N. N.; Gerges, A.; Clifford, T.; Danby, A.; Bowman-James, K. *Inorg. Chem.* **1999**, *38*, 5633.
(6) Lindoy, L. F. *The Chemistry of Macrocyclic Ligand Complexes*; Cambridge University Press: Cambridge, 1989.
(7) Blake, A. J.; Champness, N. R.; Hubberstey, P.; Li, W. S.; Schröder, M.; Withersby, M. A. *Coord. Chem. Rev.* **1999**, *183*, 117.
(8) Garcia-España, E.; LaTorre, J.; Luis, S. V.; Miravet, J. F.; Pozuelo, P.; Ramirez, J. A.; Soriano, C. *Inorg. Chem.* **1996**, *35*, 4591.
(9) Kaden, T. A.; Tschudin, D.; Studer M.; Brunner, U. *Pure Appl. Chem.* **1989**, *61*, 879.
(10) Nelson,. J.; McKee, V.; Morgan, G. In *Progress in Inorganic Chemistry*; Karlin, K. D., Ed.; Wiley: New York, 1998; Vol. 47, p 167.
(11) Nation, D. A.; Martell, A. E.; Carroll, R. I.; Clearfield A. *Inorg. Chem.* **1996**, *35*, 7246.
(12) Dobler, M. *Ionophores and their Structure*; Wiley-Interscience Publication, New York, 1981.
(13) Amendola, V.; Fabbrizzi, L.; Mangano, C.; Pallavicini, P.; Perotti, A.; Taglietti, A. *J. Chem. Soc, Dalton Trans.* **2000**, 185.
(14) Gokel, G. W. *Crown Ethers and Cryptands*; Stoddart, J. F., Ed.; The Royal Society of Chemistry: Cambridge, U.K., 1991.
(15) Lehn, J. M. *Supramolecular Chemistry*; VCH: New York, 1995.
(16) Alcock, N. W.; Curzon, E. W.; Moore, P. *J. Chem. Soc., Dalton Trans.* **1984**, 605.
(17) Guerriero, P.; Tamburini, S.; Vigato, P. A. *Coord. Chem. Rev.* **1995**, *110*, 17.
(18) Wieghardt, K.; Kleine-Boymann, M.; Nuber, B.; Weiss, J.; Zsolnai, L.; Huttner, G. *Inorg. Chem.* **1986**, *25*, 1647.
(19) Drew, M. G. B.; Rodgers, A.; McCann, M.; Nelson, S. M., *J. Chem. Soc., Chem. Commun.* **1978**, 415.
(20) Hancock, R. D.; Shaikjee, M. S.; Dobson, S. M.; Boeyens, C. A. *Inorg. Chim. Acta* **1988**, *154*, 229.
(21) Thöm, V. J.; Shaikjee, M. S.; Hancock, R. D. *Inorg. Chem.* **1986**, *25*, 2992.
(22) Thöm, V. J.; Hosken; G. D.; Hancock, R. D. *Inorg. Chem.* **1985**, *24*, 3378.
(23) Thöm, V. J.; G. D.; Hancock, R. D. *J. Chem. Soc., Dalton Trans.* **1985**, 1877.
(24) Andres, A.; Bencini, A.; Charachalios, A.; Bianchi, A.; Dapporto, P.; Garcia-España, E.; Paoletti, P.; Paoli, P. *J. Chem. Soc., Dalton Trans.* **1993**, 3507.
(25) Bencini, A.; Bianchi, A.; Castello, M.; Di Vaira, M.; Faus, J.; Garcia-España, E.; Micheloni, M.; Paoletti, P. *Inorg. Chem.* **1989**, *28*, 347.
(26) Bazzicalupi, C.; Bencini, A.; Fusi, V.; Giorgi, C.; Paoletti, P.; Valtancoli, B. *J. Chem. Soc., Dalton Trans.* **1999**, 393.
(27) Bazzicalupi, C.; Bencini, A.; Bianchi, A.; Fusi, V.; Giorgi, C.; Paoletti, P. *J. Org. Chem.* **2000**, *65*, 7686.
(28) Lodeiro, C.; Parola, A. J.; Pina, F.; Bazzicalupi, C.; Bencini, A.; Bianchi, A.; Giorgi, C.; Masotti, A.; Paoletti, P.; Valtancoli, B. *Inorg Chem.* **2001**, *40*, 2968.

10.1021/ic010597z CCC: $20.00

aromatic nitrogens whose unshared electron pairs may act cooperatively in binding cations. While in **L1** and **L2** the disposition of the heteroaromatic and aliphatic nitrogen donors is convergent toward the macrocyclic cavity, in **L3** the two aromatic nitrogens point outside the cavity. This particular molecular architecture defines two well-separated binding zones, the macrocyclic cavity and the external dipyridine unit, which can act as potential metal binding sites. Actually, a previous study on Zn(II) binding by **L3** showed that both these units could bind this metal, depending on the protonation degree of the complexes.[28]

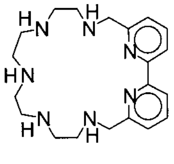

L1

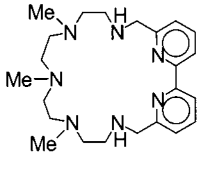

L2

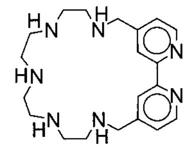

L3

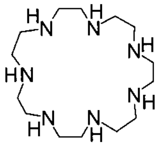

L4

Aiming to elucidate the relationship between the structural features of these ligands and their coordination properties toward Cd(II) and Pb(II), we have carried out a potentiometric, microcalorimetric, and spectrophotomeric (UV−vis) study on the interaction with these metals in aqueous solutions. The results are compared with those previously obtained with saturated polyazacycloalkanes not containing the dipyridine moiety, such as **L4**.

Results and Discussion

Ligands Protonation. The protonation features of **L1** and **L3** have been previously reported.[28] It was found that the first protonation steps take place on the aliphatic amine groups, as expected considering the higher proton affinity of aliphatic amines with respect to the heteroaromatic nitrogens of dipyridine.[29] In particular, protonation of the dipyridine nitrogens takes place in the fifth and in the third protonation step of **L1** and **L3**, respectively.[28] Protonation of the heteroaromatic nitrogens can be easily monitored by using UV−vis spectrophotometric titrations, since protonation of dipyridine is accompanied by the appearance in the UV−vis spectra of a new red-shifted band at ca. 305 nm. **L2** shows an almost equal behavior with respect to **L1**. In fact, the free amine **L2** displays a band in the UV−vis spectrum at 288 nm and binding of the first four protons does not change these spectral features. The formation of the pentaprotonated [H$_5$**L2**]$^{5+}$ species, instead, is accompanied by the appearance of a new band at 305 nm, indicating that this protonation step occurs on the heteroaromatic moiety.

The thermodynamic parameters for **L1**, **L2**, and **L3** protonation, first determined in this work, are as expected for polyamine macrocyclic compounds[29] and are reported within the Supporting Information.

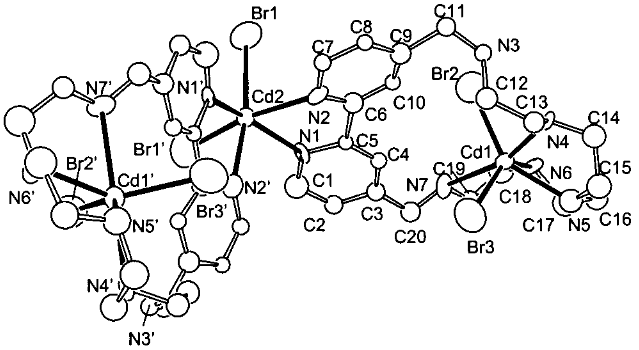

Figure 1. ORTEP drawing of the [Cd$_3$(**L3**)$_2$Br$_6$] complex.

Table 1. Selected Bond Lengths (Å) and Angles (deg) for [Cd$_3$(**L3**)$_2$Br$_6$]

Cd1−N5	2.37(3)	Cd2−N1	2.39(2)
Cd1−N6	2.41(3)	Cd2−N1′	2.39(2)
Cd1−N4	2.42(3)	Cd2−N2	2.46(3)
Cd1−Br3	2.602(6)	Cd2−N2′	2.46(3)
Cd1−N7	2.64(3)	Cd2−Br1	2.668(5)
Cd1−Br2	2.653(6)	Cd2−Br1′	2.668(5)
N5−Cd1−N6	73.7(9)	N1−Cd2−N1′	149.0(10)
N5−Cd1−N4	74.2(9)	N1−Cd2−N2	69.6(8)
N6−Cd1−N4	117.4(9)	N1′-Cd2−N2	89.9(8)
N5−Cd1−Br3	87.8(7)	N1−Cd2−N2′	89.9(8)
N6−Cd1−Br3	135.2(7)	N1′-Cd2−N2′	69.6(8)
N4−Cd1−Br3	94.9(5)	N2−Cd2−N2′	98.3(11)
N5−Cd1−N7	121.6(9)	N1−Cd2−Br1	94.5(6)
N6−Cd1−N7	70.9(9)	N1′-Cd2−Br1	105.5(6)
N4−Cd1−N7	164.2(8)	N2−Cd2−Br1	164.0(6)
Br3−Cd1−N7	86.2(6)	N2′-Cd2−Br1	83.3(6)
N5−Cd1−Br2	144.0(7)	N1−Cd2−Br1′	105.5(6)
N6−Cd1−Br2	89.5(6)	N1′-Cd2−Br1′	94.5(6)
N4−Cd1−Br2	86.5(5)	N2−Cd2−Br1′	83.3(6)
Br3−Cd1−Br2	124.6(2)	N2′-Cd2−Br1′	164.0(6)
N7−Cd1−Br2	80.0(6)	Br1−Cd2−Br1′	99.7(3)

Cd(II) Complexation. Crystal Structure of [Cd$_3$(L3)$_2$Br$_6$]·3H$_2$O. The crystal structure consists of [Cd$_3$(**L3**)$_2$Br$_6$] trinuclear complexes and water molecules. An ORTEP[30] drawing of the complex is shown in Figure 1, and Table 1 lists selected bond angles and distances for the metal coordination environments. Each trinuclear complex contains two symmetry-related [Cd**L3**Br$_2$] moieties (symmetry operation: $1 - x, y, 0.5 - z$), with the cadmium atom lodged inside the macrocyclic cavity, coordinated to four nitrogens of the aliphatic chain and two bromide anions. The two [Cd**L3**Br$_2$] units are joined together by the third cadmium (Cd2), which lies on a C_2 crystallographic axis. Actually, the Cd2 is coordinated by the nitrogen atoms of the dipyridine moieties belonging to the symmetry-related ligand molecules and by two bromide ions (Br1 and Br1′). The coordination geometry can be best described as a distorted octahedron, with the two bromide anions in cis position. Although the pyridine rings of each dipyridine moiety are not coplanar (dihedral angle 16.3(8)°), the coordination bite of the dipyridine unit gives rise to a small N1−Cd2−N2 angle (69.6(8)° vs the theoretical 90° one). This leads to an overall distorted octahedral geometry; N1, N2, N1′, and Br1′ define the equatorial plane, while N2′ and Br1 occupy the axial positions. However, because of the crystallographic symmetry, the equatorial plane can be also defined by N2′, N1′, N1, and Br1 with N2 and Br1′ in the axial positions.

Cd1 is hexacoordinated by four nitrogen atoms of the aliphatic chain (N4, N5, N6, and N7) and by the Br2 and Br3 bromide anion. The nitrogen donor N7, however, coordinates to the metal at a longer distance. The coordination environment can be best described as a distorted trigonal prism, with the basal planes

---

(29) Bencini, A.; Bianchi, A.; Garcia-España, E.; Micheloni, M.; Ramirez, J. A. *Coord. Chem. Rev.* **1999**, *118*, 97.

(30) Johnson, C. K.; Burnett, M. N. ORTEP-3. Windows version by L. Farrugia. *J. Appl. Crystallogr.* **1996**, *30*, 565.

Table 2. Formation Constants and Corresponding Thermodynamic Parameters (kJ · mol^{-1}) for the Cd(II) Complexes with Ligands **L1**−**L3** (0.1 M NMe_4Cl, 298.1 K)

	log *K*	−Δ*G*°	−Δ*H*°	*T*Δ*S*°
	L = **L1**			
$Cd^{2+} + L = CdL^{2+}$	15.69(3)[a]	89.4	28.0(4)	61.4(4)
$CdL^{2+} + H^+ = CdLH^{3+}$	5.22(3)	29.7	34.0(4)	−4.3(4)
$CdLH^{3+} + H^+ = CdLH_2^{4+}$	4.90(4)	27.9	33.7(4)	−5.8(4)
$CdLH_2^{4+} + H^+ = CdLH_3^{5+}$	3.74(4)	21.3	28.4(4)	−7.1(4)
	L = **L2**			
$Cd^{2+} + L = CdL^{2+}$	13.23(2)	75.3	19.6(2)	55.7(2)
$CdL^{2+} + H^+ = CdLH^{3+}$	6.05(2)	34.5	37.5(3)	−3.0(3)
$CdLH^{3+} + H^+ = CdLH_2^{4+}$	5.41(3)	30.9	45.6(2)	−14.7(2)
	L = **L3**			
$Cd^{2+} + L = CdL^{2+}$	7.7(1)	43.9	19.2(2)	24.7(2)
$CdL^{2+} + H^+ = CdLH^{3+}$	8.38(9)	47.8	27.8(2)	20.0(2)
$CdLH^{3+} + H^+ = CdLH_2^{4+}$	6.77(8)	38.6	21.6(2)	17.0(2)
$CdLH_2^{4+} + H^+ = CdLH_3^{5+}$	5.30(8)	30.2	26.7(3)	3.5(3)
$CdLH_3^{5+} + H^+ = CdLH_4^{6+}$	4.09(8)	23.3	29.7(3)	−6.4(3)
	L = **L4**[b]			
$Cd^{2+} + L = CdL^{2+}$	18.10	103.3	67.3	36.0

[a] Values in parentheses are standard deviations on the last significant figure. [b] Values from ref 25.

defined by Br2, N6, N7 and by N4, N5, Br3, respectively. The nitrogen N3 is not involved in metal coordination

The overall conformation of the $[Cd_3(\mathbf{L3})_2Br_6]$ complex is rather bent with an angle of 59.53(3)° between the Cd1⋯Cd2 and Cd2⋯Cd1′ internuclear distances.

Cd(II) Coordination in Aqueous Solution. Cd(II) coordination by ligands **L1**−**L3** was studied by means of potentiometric and microcalorimetric measurements, and the thermodynamic parameters for the formation of the complexes in aqueous solutions are listed in Table 2, together with those previously found for **L4**.[25]

Considering the data in Table 2, some general features can be outlined. First, all ligands form mononuclear [Cd**L**]$^{2+}$ complexes (**L** = **L1**−**L3**) in aqueous solutions. The data analysis with the program HYPERQUAD[31] under our experimental conditions revealed 1:1 stoichiometries for all the species detected. The stability constants of the **L1**−**L3** complexes, however, are rather low considering the large number of nitrogen atoms which could be involved in metal coordination.[2,9,25,26] Second, Cd(II) forms stable complexes with protonated species of the ligands. This tendency is particularly evident in the case of **L3**, which can form up to a tetraprotonated [Cd**L3**H$_4$]$^{6+}$ complex. Consequently, protonated species of the complexes are present in solution from acidic to neutral pH values (Figure S1, Supporting Information).

It can be of interest to compare the stability constants of the present mononuclear complexes with those of the Cd(II) complexes with the macrocyclic ligand 1,4,7,10,13,16,19-heptaazacycloheneicosane (**L4**),[25] which contains seven secondary amine groups linked by ethylenic chains. In particular, the formation constants of the **L1** and **L2** complexes are lower than the **L4** one (log *K* = 15.70 and 13.23 for [Cd**L1**]$^{2+}$ and [Cd**L2**]$^{2+,}$ respectively, vs log *K* = 18.10 for [Cd**L4**]$^{2+}$, Table 2). Such a different stability cannot be simply related to the different binding properties of dipyridine with respect to an ethylenediamine unit, since 2,2′-dipyridine and *N*,*N*′-dimethylethylenediamine show almost equal binding abilities toward Cd(II) (log *K* = 4.6 and 5.2 for the equilibrium $Cd^{2+} + \mathbf{L} = [Cd\mathbf{L}]^{2+}$ with **L** = 2,2′-dipyridine and *N*,*N*′-dimethylethylenediamine, respectively).[32] The lower stability of the **L1** and **L2** complexes can be explained instead considering the formation of one or more large chelate rings due to the presence of some nitrogen donors not bound to the metal. Most likely, as previously found in phenanthroline-containing macrocycles,[33−36] the rigidity of the dipyridine unit does not allow the simultaneous involvement in metal binding of the heteroaromatic nitrogens and the adjacent benzylic amine groups. This hypothesis is supported by the high values of the equilibrium constants for successive addition of H$^+$ to the [Cd**L1**]$^{2+}$ and [Cd**L2**]$^{2+}$ complexes, which suggest that protonation takes place on uncoordinated nitrogen atoms. Furthermore, the enthalpy changes for Cd(II) complexation with **L1** and **L2** are remarkably lower than those found for **L4**,[25] indicating that the overall interaction between Cd(II) and **L4** is stronger than that between Cd(II) and **L1** or **L2** (Table 2). The large enthalpy increment can arise from the larger flexibility of the **L4** macrocyclic ring, which may allow the nitrogen donors to achieve an optimal arrangement around the metal ion, forming strong Cd(II)−N bonds. On the contrary, the entropy changes for Cd(II) complexation are more favorable for **L1** and **L2** with respect to **L4**. Two main factors can be invoked to rationalize this aspect. First, **L1** and **L2** present a more rigid structure, with a consequent lower entropic cost for the process of ligand rearrangement upon metal complexation. Second, complexes with primary or secondary amines are normally more solvated than complexes with tertiary or heteroaromatic ones, due to the inability of the latter to give N−H⋯OH$_2$ hydrogen bonds. This may result in a larger desolvation of ligands **L1** and **L2** upon metal complexation, leading to a more favorable entropic contribution with respect to **L4**.

The comparison of the **L1** and **L2** thermodynamic data in Table 2 points out that the lower stability of the Cd(II) complex with **L2** is mainly due to a less favorable enthalpic contribution. *N*-Methylation, in fact, reduces the σ-donating properties of the amine groups, due to the absence of M−N−H⋯O hydrogen bonds to the solvent, that make them weaker σ-donors.[37,38] Furthermore, steric hindrance due to the insertion of methyl groups within the ligand framework can cause elongation of the M−N bonds as well as distortions of the coordination sphere of the metal in its complexes, thus reducing the overall metal−ligand interaction.

Considering ligand **L3**, the crystal structure of the $[Cd_3(\mathbf{L3})_2Br_6]$ complex outlines that this ligand contains two well-separated binding units for the metal ion, i.e., the macrocyclic cavity and the external dipyridine nitrogens. On the other hand, only 1:1 Cd(II) complexes are formed in aqueous solutions. The most significant differences in Cd(II) coordination between ligands **L1**, **L2**, and **L3** are the marked lower stability of the [Cd**L3**]$^{2+}$ complex and its tendency to form highly protonated species in aqueous solution (Table 2). The first three protonation

---

(31) Gans, P.; Sabatini, A.; Vacca, A. *Talanta* **1996**, *43*, 807.

(32) Smith, R. M.; Martell, A. E. *NIST Stability Constants Database*, version 4.0; National Institute of Standards and Technology: Washington, DC, 1997.

(33) Bazzicalupi, C.; Bencini, A.; Fusi, V.; Giorgi, C.; Paoletti, P.; Valtancoli, B. *Inorg. Chem.* **1998**, *37*, 941.

(34) Chand, D. K.; Schneider, H.-J.; Bencini, A.; Bianchi, A.; Giorgi, C.; Ciattini, S.; Valtancoli, B. *Chem. Eur. J.* **2000**, *6*, 4001.

(35) Bazzicalupi, C.; Bencini, A.; Bianchi, A.; Fusi, V.; Giorgi, C.; Paoletti, P.; Valtancoli, B.; Pina, F.; Bernardo, M. A. *Inorg. Chem.* **1999**, *37*, 3806.

(36) Bazzicalupi, C.; Bencini, A.; Bianchi, A.; Fusi, V.; Giorgi, C.; Paoletti, P.; Valtancoli, B.; Pina, F.; Bernardo, M. A. *Eur. J. Inorg. Chem.* **1999**, 1911.

(37) Golub, G.; Cohen H.; D. Meyerstein, *J. Chem. Soc., Chem. Commun.* **1992**, 398.

(38) Golub, G.; Cohen H.; Paoletti, P.; Bencini, A.; Messori, L.; Bertini, I.; Meyerstein, D. *J. Am. Chem. Soc.* **1995**, *117*, 8353.

constants of the complex are remarkably higher than that reported for 2,2′-dipyridine alone (log $K = 4.39$),[32] suggesting that at least in $[\mathrm{Cd}\mathbf{L3}\mathrm{H}_3]^{5+}$ the three acidic protons are located on the polyamine chain. These data may indicate that in the protonated Cd(II) complexes the metal ion is located outside the cavity, coordinated by the heteroaromatic nitrogen donors of dipyridine, as already found in the case of the protonated Zn(II) complexes with this ligand.[28] On the other hand, the stability constant of the $[\mathrm{Cd}\mathbf{L3}]^{2+}$ is by far higher than those reported for the Cd(II) complex with 2,2′-dipyridine (log $K = 7.7$ for $[\mathrm{Cd}\mathbf{L3}]^{2+}$ vs log $K = 4.25$ for $[\mathrm{Cd}(2,2'\text{-dipyridine})]^{2+}$),[32] suggesting that in the $[\mathrm{Cd}\mathbf{L3}]^{2+}$ complex the metal is lodged inside the macrocyclic cavity.

Comparing the thermodynamic contributions to Cd(II) complexation with **L1**−**L3**, the less favorable enthalpic and entropic contributions to the stability of the $[\mathrm{Cd}\mathbf{L3}]^{2+}$ complex with respect to the **L1** and **L2** ones can be explained by considering the lower number of nitrogen donors available for the coordination of the metal inside the **L3** macrocyclic cavity and the consequently reduced desolvation of the metal ion. Actually, the crystal structure of the $[\mathrm{Cd}_3(\mathbf{L3})_2\mathrm{Br}_6]$ complex shows that the metal enclosed in the macrocyclic cavity (Cd1) is coordinated just by four nitrogen donors and completes its coordination environment with two bromide anions. Most likely, these anions are replaced by water molecules in aqueous solutions.

In order to further clarify the coordination features of these ligands, we carried out a UV−vis spectrophotometric study on solutions containing Cd(II) and ligands **L1**−**L3** in equimolecular ratio. As previously anticipated, ligands **L1** and **L2** present a sharp band at 288 nm in their UV spectra ($\epsilon = 11700$ and 12200 $\mathrm{mol^{-1}\ dm^3\ cm^{-1}}$, respectively). Similarly the UV spectrum of **L3** shows a band at 283 nm ($\epsilon = 11950\ \mathrm{mol^{-1}\ dm^3\ cm^{-1}}$). As previously observed in the case of proton and Zn(II) binding,[28] Cd(II) coordination by the heteroaromatic unit gives marked changes in the absorption spectra of ligands **L1**−**L3**, with the appearance of new red-shifted absorption bands at 304 nm for **L1** and **L2** and 298 nm for **L3** ($\epsilon = 14030$, 13770, and 15340 $\mathrm{mol^{-1}\ dm^3\ cm^{-1}}$, respectively). These new bands can be used as a diagnostic tool to prove the effective involvement of dipyridine in metal binding. In the case of the **L1** and **L2** complexes, these spectral features do not vary significantly in the pH range 11−4, where the $[\mathrm{Cd}\mathbf{L}]^{2+}$ ($\mathbf{L} = \mathbf{L1}$ or $\mathbf{L2}$) complexes or their mono- and diprotonated forms are the main species present in solution. Therefore, in the Cd(II) complexes with **L1** or **L2** the metal is coordinated to the heteroaromatic nitrogens of the dipyridine unit, inside the macrocyclic cavity.

A different behavior is found for the Cd(II) complex with **L3**. Figure 2 displays the molar absorbance values at 298 nm for the **L3** complexes as a function of pH. The comparison of the spectrophotometric titration curve with the distribution diagram of the protonated and complexed species of **L3** (Figure 2) clearly shows a marked decrease of the absorbance at 298 nm in the pH range 2−5. In this pH range highly protonated species of the ligand are prevalent in aqueous solution and the decrease in absorbance is mainly due to partial deprotonation of the dipyridine unit passing from $[\mathrm{H}_5\mathbf{L3}]^{5+}$ to $[\mathrm{H}_3\mathbf{L3}]^{3+}$, as already observed in the spectrophotometric titration of the ligand alone.[28] Above pH 5 the formation of the diprotonated species of the complex $[\mathrm{Cd}\mathbf{L3}\mathrm{H}_2]^{4+}$ gives rise, once again, to an increase of the absorbance. These data account for the involvement of the dipyridine unit in metal coordination in the protonated forms of this Cd(II) complex. In other words, in the protonated complexes, the metal is lodged outside the cavity, coordinated by the heteroaromatic nitrogens, while the acidic protons are bound by the polyamine chain (Scheme 1).

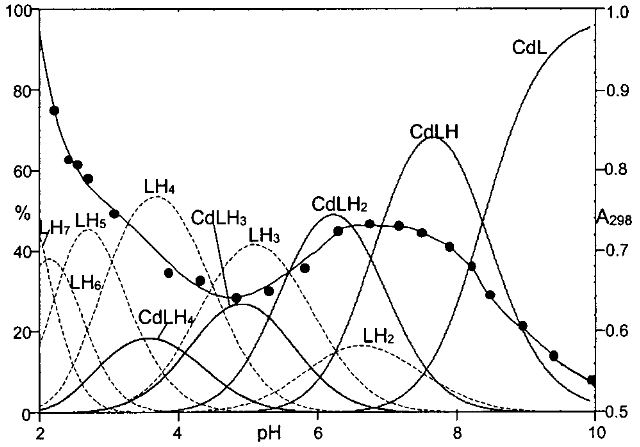

Figure 2. Absorbance at 298 nm (●) and percentages of the protonated (dashed lines) and complexed (solid lines) species of **L3** in the presence of Cd(II) (1:1 molar ratio) as a function of pH ($[\mathbf{L3}] = [\mathrm{Cd(II)}] = 6.7 \times 10^{-5}$ M, $I = 0.1$ M).

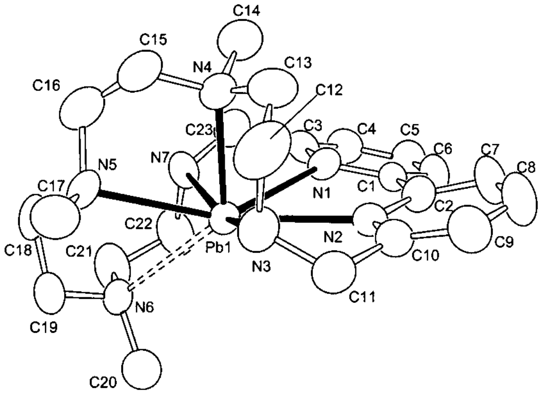

Figure 3. ORTEP drawing of the $[\mathrm{Pb}\mathbf{L2}]^{2+}$ cation.

Scheme 1

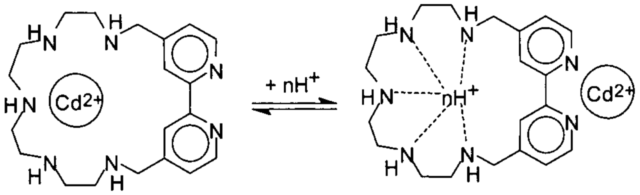

The most interesting finding, however, is the sharp decrease of the absorbance at alkaline pH's, occurring upon the formation of the $[\mathrm{Cd}\mathbf{L3}]^{2+}$ complex. Such a behavior implies that in the nonprotonated form of the complex the dipyridine unit is not involved in metal coordination and Cd(II) is lodged inside the macrocyclic cavity. Therefore, the particular molecular topology of this ligand gives rise to a pH-controlled translocation of the metal, since protonation of the $[\mathrm{Cd}\mathbf{L3}]^{2+}$ complex leads to a "jump" of the metal cation from inside to outside the cavity (Scheme 1).

Pb(II) Complexation. Crystal Structure of $[\mathrm{Pb}\mathbf{L2}](\mathrm{BPh}_4)_2$. The crystal structure of $[\mathrm{Pb}\mathbf{L2}](\mathrm{BPh}_4)_2$ contains $[\mathrm{Pb}\mathbf{L2}]^{2+}$ complexed cations and tetraphenylborate anions. Figure 3 shows an ORTEP[30] drawing of the cation with atom labeling. Table 3 lists selected bond lengths and angles for metal coordination environment.

The metal ion is heptacoordinated by the nitrogen atoms of the macrocycle. The bond lengths range from 2.551(9) Å for

Table 3. Selected Bond Lengths (Å) and Angles (deg) for $[Pb\mathbf{L3}](BPh_4)_2$

Pb1−N4	2.551(9)	Pb1−N7	2.752(8)
Pb1−N5	2.715(9)	Pb1−N1	2.787(8)
Pb1−N3	2.725(9)	Pb1−N6	2.906(9)
Pb1−N2	2.749(8)		
N4−Pb1−N5	69.9(3)	N5−Pb1−N1	139.5(2)
N4−Pb1−N3	68.3(3)	N3−Pb1−N1	117.7(3)
N5−Pb1−N3	86.0(3)	N2−Pb1−N1	59.2(2)
N4−Pb1−N2	86.2(3)	N7−Pb1−N1	62.5(3)
N5−Pb1−N2	146.1(3)	N1−Pb1−N6	114.2(3)
N3−Pb1−N2	62.4(3)	N2−Pb1−N6	143.2(3)
N4−Pb1−N7	94.7(3)	N3−Pb1−N6	125.1(3)
N5−Pb1−N7	85.2(3)	N4−Pb1−N6	130.5(3)
N3−Pb1−N7	162.7(3)	N5−Pb1−N6	64.8(3)
N2−Pb1−N7	121.6(2)	N6−Pb1−N7	63.4(3)
N4−Pb1−N1	88.1(3)		

Pb−N4 to 2.906(9) Å for Pb−N6 (see Table 3). The rather high value of the Pb−N6 bond distance indicates a weak interaction of this nitrogen with the metal. The coordination geometry can be described as a distorted capped trigonal prism, with the two bases defined by N1, N2, and N6 and by N3, N4, and N5, respectively. N7 caps the N1−N4−N5−N6 face of the trigonal prism. The resulting arrangement for the seven donor atoms around the lead ion leaves a zone free from coordinated donor atoms, which is occupied by the lone pair of Pb^{2+}. Such a "gap" in the coordination geometry has been ascribed by several authors to the presence of a stereochemically active lone pair.[20−23,39,40] The Pb−N4 bond is placed on the side opposite to the vacant zone, and its length (2.551(2) Å) is in agreement with the values reported for complexes where the lone pair is active (2.37−2.56 Å).[20−24,26]

As shown in Figure 3, the macrocyclic ligand assumes a folded conformation, which allows the ligands to "wrap" around the metal and all seven nitrogens to interact with the Pb^{2+} ion. Only the zone occupied by the stereochemically active lone pair of the metal seems to be apparently less crowded by the ligand.

Considering the overall conformation of the ligand and the disposition of the donor atoms around the metal, closest comparisons can be found in the crystal structure of the Pb(II) complex with ligand 2,5,8,11,14-pentaaza[15]-[15](2,9)[1,10]-phenanthrolinophane, which contains a pentaamine chain linking the 2,9 positions of phenanthroline.[26] In this complex the metal is heptacoordinated by the seven nitrogen donors, the most significant difference being the remarkably longer distances found for the Pb−N bonds (four of them range between 2.75 and 2.9 Å). In the present $[Pb\mathbf{L2}]^{2+}$ complex the nitrogen donors seem to achieve a better arrangement around the metal ion, probably due to the presence in **L2** of a more flexible heteroaromatic unit, as testified by the dihedral angle of 24.4(3)° formed between the planes containing the two aromatic rings.

Pb(II) Coordination in Aqueous Solution. As usually observed in Cd(II) and Pb(II) complexation by polyamines,[3,20,24−26,32] the stability of the Pb(II) complexes with ligands **L1** and **L2** is lower than that of the Cd(II) ones. As shown in Tables 2 and 4 this is mainly due to more favorable entropic contributions to the stability of the Cd(II) complexes. On the contrary, the enthalpic terms ($-\Delta H°$) are higher for the Pb(II) complexes. These experimental observations can be explained by considering the "soft" nature of Pb(II), which may give rise to metal−ligand interaction with a larger covalent contribution, thus increasing the enthalpic contribution to the complex stability with respect to the smaller Cd(II) ion. At the same time, Pb(II) complexation by polyamines is often accompanied by remarkable rearrangements of the ligand around the metal, as actually shown, in the present case, by the crystal structure of the $[Pb\mathbf{L2}]^{2+}$ complex. This may decrease the entropic contribution to the process of complex formation.

Table 4. Formation Constants and Corresponding Thermodynamic Parameters (kJ · mol^{-1}) for the Pb(II) Complexes with Ligands **L1**−**L3** (0.1 M NMe_4Cl, 298.1 K)[a]

	log *K*	$-\Delta G°$	$-\Delta H°$	$T\Delta S°$
	L = **L1**			
$Pb^{2+} + L = PbL^{2+}$	12.96(4)[b]	74.0	36.4(2)	37.6(2)
$PbL^{2+} + H^+ = PbLH^{3+}$	6.20(4)	35.1	30.5(4)	4.6(4)
$PbLH^{3+} + H^+ = PbLH_2^{4+}$	5.92(6)	33.9	40.5(2)	−6.3(2)
$PbLH_2^{4+} + H^+ = PbLH_3^{5+}$	3.92(6)	22.6	34.3(5)	−11.7(5)
	L = **L2**			
$Pb^{2+} + L = PbL^{2+}$	11.51(3)	65.6	25.5(1)	40.1(1)
$PbL^{2+} + H^+ = PbLH^{3+}$	5.87(4)	33.4	34.7(1)	−1.2(1)
$PbLH^{3+} + H^+ = PbLH_2^{4+}$	5.02(4)	28.8	35.9(2)	−7.1(2)
	L = **L3**			
$Pb^{2+} + L = PbL^{2+}$	9.63(8)	54.8	31.3(4)	23.5(4)
$PbL^{2+} + H^+ = PbLH^{3+}$	7.0(1)	39.7	38.5(4)	1.2(4)
$PbLH^{3+} + H^+ = PbLH_2^{4+}$	5.9(1)	33.8	40.5(4)	−6.7(4)
$PbLH_2^{4+} + H^+ = PbLH_3^{5+}$	5.4(1)	30.9	21.7(3)	9.0(3)
$PbL^{2+} + OH^- = PbL(OH)^+$ [c]	4.3(1)			

[a] Log $K = 10.02$ for $Pb^{2+} + \mathbf{L4} = Pb\mathbf{L4}^{2+}$ (from ref 24). [b] Values in parentheses are standard deviations on the last significant figure. [c] The enthalpy change for $PbL(OH)^+$ could not be determined, due to precipitation at alkaline pH's in the conditions used in the microcalorimetric measurements.

Similarly to Cd(II), the $[Pb\mathbf{L1}]^{2+}$ and $[Pb\mathbf{L2}]^{2+}$ complexes show a marked tendency to protonate. The values of the protonation constants and the corresponding highly favorable enthalpic contributions suggest that some nitrogen donors are not involved, or weakly involved in metal coordination. This hypothesis is confirmed, once again, by the crystal structure of the $[Pb\mathbf{L2}]^{2+}$ complex, which displays one of the aliphatic nitrogens weakly bound to the metal ion.

Differently from Cd(II), both **L1** and **L2** form more stable Pb(II) complexes than **L4** (log K = 12.96 and 11.51 for $[Pb\mathbf{L1}]^{2+}$ and $[Pb\mathbf{L2}]^{2+}$, respectively, Table 4, vs log K = 10.02[24] for $[Pb\mathbf{L4}]^{2+}$). This fact may be related to the insertion of a dipyridine moiety within the macrocyclic framework. In order to get further information on the role played by the dipyridine unit in the Pb(II) coordination, the reaction of complex formation was followed by means of UV spectra recorded on aqueous solutions containing the $[Pb\mathbf{L1}]^{2+}$ and $[Pb\mathbf{L2}]^{2+}$ complexes. As already observed in the Cd(II) complexes, Pb(II) complexation by **L1** and **L2** gives rise to a new red-shifted band at 302 nm for $[Pb\mathbf{L1}]^{2+}$and 304 nm for $[Pb\mathbf{L2}]^{2+}$ (ϵ = 13000 and 13120 mol^{-1} dm^3 cm^{-1}, respectively). These spectral data account for the involvement of the dipyridine moiety in metal coordination in the $[Pb\mathbf{L}]^{2+}$ complexes (**L** = **L1** or **L2**) in aqueous solution. This suggestion is further confirmed by the crystal structure of the $[Pb\mathbf{L2}](BPh_4)_2$ complex, which shows that both the aromatic nitrogens are bound to the metal. Most likely, the different stability of the Pb(II) complexes with the dipyridine-containing **L1** and **L2** and the aliphatic **L4** macrocycle is due to the replacement in the metal coordination sphere of two coordinating amine groups in the **L4** complex with the heteroaromatic nitrogens in the **L1** and **L2** complexes; the latter donor atoms are known to show a better coordination ability toward large and "soft" metal cation, such as Pb(II).

---

(39) Byriel, K.; Dunster, K. R.; Gahan, L. R.; Kennard, C. H. L.; Latten, J. L.; Swann, I. L.; Duckworth, P. A. *Polyhedron* **1992**, *10*, 1205.

(40) Shimoni-Livny, L.; Glusker, J. P.; Bock, C. W. *Inorg. Chem.* **1998**, *37*, 1853.

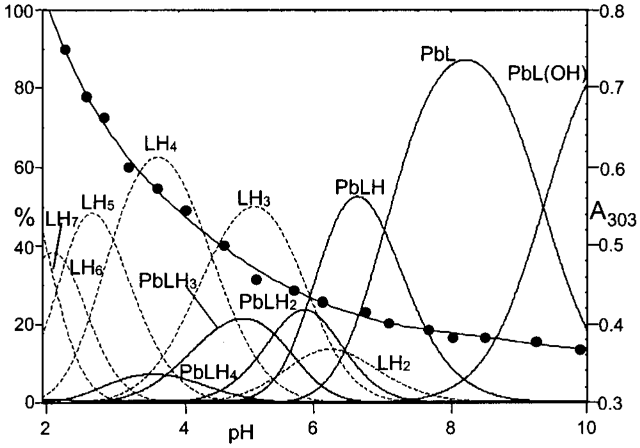

Figure 4. Absorbance at 303 nm (●) and percentages of the protonated (dashed lines) and complexed (solid lines) species of **L3** in the presence of Pb(II) (1:1 molar ratio) as a function of pH ([**L3**] = [Pb(II)] = 6.2×10^{-5} M, $I = 0.1$ M).

Ligand **L3** displays a different coordination behavior toward Pb(II). The comparison of the data in Tables 2 and 4 clearly shows that the Pb(II) complex with **L3** is more stable than the corresponding complex with Cd(II), that is the opposite behavior found for the **L1** and **L2** complexes. The entropic contributions to Cd(II) and Pb(II) complexation with **L3** are almost equal, the higher stability of the [Pb**L3**]$^{2+}$ complex being due to a more favorable enthalpic term, which can be related, once again, to the softer character of Pb(II) and to the consequent increase of the covalent nature of the Pb−N bonds.

As in the case of the Cd(II) complex, the [Pb**L3**]$^{2+}$ complex forms several protonated species in aqueous solution. It should be noted, however, that the protonation constants of [Pb**L3**]$^{2+}$ are by far lower than those of the [Cd**L3**]$^{2+}$ complex. In order to ascertain the effective role of the heteroaromatic nitrogens in Pb(II) complexation by ligand **L3**, we carried out a spectrophotometric study on its complexes. As previously anticipated, Pb(II) complexation by **L1** and **L2** gives rise to new red-shifted bands at ca. 303 nm. This spectral feature does not change in the protonated species of the complexes, indicating that protonation takes place on aliphatic amine groups. On the contrary, Pb(II) complexation by **L3** does not change significantly the UV spectrum of the ligand. Figure 4 shows the absorbance at 303 nm at different pH values for a system containing Pb(II) and **L3** in 1:1 molar ratio. The band at 303 nm observed at strongly acidic pH values is due to the presence in solution of polyprotonated species of the ligand and disappears with the formation of the Pb(II) complexes from slightly acidic to alkaline pH values. Therefore, in the protonated Pb(II) complexes as well as in the [Pb**L3**]$^{2+}$ complex the metal is coordinated inside the macrocyclic cavity.

Conclusions

Both Cd(II) and Pb(II) form 1:1 complexes in aqueous solutions with ligands **L1** and **L2**, which contain similar polyamine chains linking the 2,2′ position of a dipyridine unit. In these complexes the metal is coordinated by the dipyridine moiety, as shown by the appearance of new red-shifted bands in the UV spectra as well as by the crystal structure of the [Pb**L2**]$^{2+}$ complex. On the other hand, the high values of the protonation constants of the complexes suggest that some aliphatic amine groups are weakly bound or not bound to the Cd(II) or Pb(II) ion. The comparison between the binding ability of **L1** and **L2** and the saturated heptaamine macrocycle **L4**, where an ethylendiamine chain replaces the dipyridine moiety, shows that both the dipyridine-containing macrocycles form less stable Cd(II) complexes than **L4**. The introduction of a rather rigid heteroaromatic unit leads to stiffening of the macrocyclic structure and does not allow an optimal arrangement of the nitrogen donors around the metal cation, thus reducing the complex stability. On the contrary, the Pb(II) complexes with **L1** and **L2** are more stable than that with **L4**, due to the better binding ability of the heteroaromatic donors toward the large and soft Pb(II) ion.

As shown by the crystal structure of the [Cd_3(**L3**)$_2Br_6$] complex, **L3** contains two well-separated binding moieties. This particular molecular architecture gives rise to a different coordination behavior toward Cd(II) and Pb(II) in aqueous solutions. In the mononuclear [Cd**L3**]$^{2+}$ complex, the metal is coordinated inside the macrocyclic cavity, not bound by the heteroaromatic moiety. Protonation of the complex takes place on the more basic aliphatic amine groups and leads to translocation of the metal from inside to outside the cavity. Therefore, in the [Cd**L3**H_n]$^{(2+n)+}$ complexes, the metal is coordinated to the heteroaromatic nitrogens. In the Pb(II) complexes the metal is lodged inside the macrocyclic cavity even in its protonated species. Such a different behavior with respect to Cd(II) can be explained considering the higher stability of the [Pb**L3**]$^{2+}$ complex than the [Cd**L3**]$^{2+}$ one.

Experimental Section

Synthesis. Ligands **L1**, **L2**, and **L3** were obtained as previously reported.[27,28]

[Cd_3(L3)$_2Br_6$]·$3H_2O$. A solution of $Cd(NO_3)_2 \cdot 4H_2O$ (10.6 mg, 0.031 mmol) in MeOH (10 cm^3) was slowly added to a methanol solution (5 cm^3) of **L3** (8.0 mg, 0.021 mmol). Sodium bromide (6.6 mg, 0.063 mmol) and butanol (10 cm^3) were then added. Colorless crystals of the complex suitable for X-ray analysis were obtained by slow evaporation at room temperature of this solution. Yield: 9 mg (55%) Elemental anal. Found: C, 30.0; H, 4.1; N, 12.4. Calcd for $C_{40}H_{68}Br_6Cd_3N_{14}O_3$: C, 29.85; H, 4.26; N, 12.18.

[PbL2](BPh_4)$_2$. A solution of $Pb(NO_3)_2$ (7 mg, 0.021 mmol) in MeOH (10 cm^3) was slowly added to a methanol solution (5 cm^3) containing **L2** (8.6 mg, 0.021 mmol). To the resulting solution were added $NaBPh_4$ (7.2 mg, 0.021 mmol) and butanol (10 cm^3). Colorless crystals of the complex suitable for X-ray analysis were obtained by slow evaporation at room temperature of this solution. Yield: 5.2 mg (60%) Elemental anal. Found: C, 67.8; H, 6.21; N, 7.82. Calcd for $C_{71}H_{77}B_2PbN_7$: C, 67.83; H, 6.17; N, 7.79.

X-ray Structure Analyses. Analyses on prismatic colorless single crystals of [Cd_3(**L3**)$_2Br_6$]·$3H_2O$ (a) and [Pb**L2**](BPh_4)$_2$ (b) were carried out with an Enraf-Nonius CAD4 X-ray diffractometer. Details for data collections and structure refinements are summarized in Table 5. Intensity data were empirically corrected for absorption (PSI-SCAN method). Both structures were solved by direct methods of the SIR97 program.[41] Refinements were performed by means of the full-matrix least-squares method of the SHELXL-97 program.[42]

X-ray Structure Determination of [Cd_3(L3)$_2Br_6$]·$3H_2O$ (a). Anisotropic displacement parameters were used for cadmium, bromine, and nitrogen atoms, except N3 and N5. All hydrogen atoms were introduced in calculated positions with fixed isotropic thermal parameters. Crystals of this compound were of rather low quality. This accounts for the high values of the agreement factors at the end of refinement and of the thermal parameters for some atoms. Several attempts to obtain crystals of better quality did not give good results. Residual electron density is present near the cadmium atoms.

---

(41) Altomare, A.; Burla, M. C.; Camalli, M.; Cascarano, G. L.; Giacovazzo, C.; Guagliardi, A.; Moliterni, A. G. G.; Polidori, G.; Spagna, R. *J. Appl. Crystallogr.* **1999**, *32*, 115.

(42) Sheldrick, G. M. *SHELXL-97*; University of Göttingen: Göttingen, 1997.

Table 5. Crystal Data and Structure Refinement for $[Cd_3(\mathbf{L3})_2Br_6]\cdot 3H_2O$ (a) and $[Pb\mathbf{L2}](BPh_4)_2$ (b)

	(a)	(b)
empirical formula	$C_{40}H_{68}Br_6Cd_3N_{14}O_3$	$C_{71}H_{77}B_2N_7Pb$
fw	1609.74	1257.21
temp, K	298	298
wavelength, Å	0.71069	0.71069
space group	$C2/c$	$P2_1/c$
a, Å	17.504(9)	11.335(5)
b, Å	21.940(1)	28.526(5)
c, Å	15.726(1)	19.635(5)
β, deg	117.37(5)	106.430(5)
vol, Å^3	5363(3)	6090(3)
Z	4	4
calcd density, Mg/m^3	1.994	1.371
abs coeff, mm^{-1}	5.699	2.819
cryst size, mm	0.35 × 0.3 × 0.1	0.25 × 0.2 × 0.2
final R indices $[I > 2\sigma(I)]^a$	R1 = 0.0972	R1 = 0.0545
	wR2 = 0.2591	wR2 = 0.1197
R indices (all data)^a	R1 = 0.2832	R1 = 0.0912
	wR2 = 0.3473	wR2 = 0.1475

[a] $R1 = \sum||F_o| - |F_c||/\sum|F_o|$; $wR2 = [\sum w(F_o^2 - F_c^2)^2/\sum wF_o^4]^{1/2}$.

X-ray Structure Determination of $[PbL2](BPh_4)_2$ (b). Anisotropic displacement parameters were used for all non-hydrogen atoms. Hydrogen atoms were introduced in calculated position and isotropically refined accordingly to the linked atoms. Residual electron density is present near the lead atom.

Potentiometric Measurements. Equilibrium constants for protonation and complexation reactions with **L1**, **L2**, and **L3** were determined by pH-metric measurements at 298.1 ± 0.1 K, by using equipment and procedures[25] which have been already described. 1×10^{-3} to 2×10^{-3} mol dm^{-3} ligands and metal ions concentrations were employed in the potentiometric measurements, varying the metal to ligand molar ratio from 0.5:1 to 2:1. Three titration experiments (about 100 data points each one) were performed in the pH range 2.5−10.5. The computer program HYPERQUAD[31] was used to calculate the equilibrium constants from the emf data.

Microalorimetric Measurements. The enthalpies of protonation and metal complexation of **L1**, **L2**, and **L3** were determined in 0.1 M NMe_4Cl aqueous solutions by means of an automated system composed of a Thermometric AB thermal activity monitor (model 2277) equipped with a perfusion-titration device and Hamilton pump (model Microlab M) coupled with a 0.250 cm^3 gastight Hamilton syringe (model 1759 LT). Typically 1.2 cm^3 of an acidic solution of ligand and metal (both 5×10^{-3} M) in 0.1 M NMe_4Cl was charged into the calorimetric ampule. After thermal equilibration, 0.015 cm^3 additions of a 0.1 M NMe_4OH standard solution were delivered. Under the reaction conditions and employing the determined protonation constant, the concentrations of the species present in solution before and after addition were calculated and the corresponding enthalpies of reaction were determined from the calorimetric data by means of the AAAL program.[43] At least three titrations were performed for each system. The titration curves for each system were treated either as a single set or as separated entities without significant variation in the values of the enthalpy changes.

Spectrophotometric Measurements. Absorption spectra were recorded on a Perkin-Elmer Lambda 9 spectrophotometer. HCl and NaOH were used to adjust the pH values that were measured on a Metrohm 713 pH meter.

Acknowledgment. Financial support by the Italian Ministero dell'Università e della Ricerca Scientifica e Tecnologica (COFIN 2000) is gratefully acknowledged.

Supporting Information Available: An X-ray crystallographic file, in CIF format. Tables listing detailed crystallographic data, atomic positional parameters, anisotropic temperature factors, and bond distances and angles for $[Cd_3(\mathbf{L3})_2Br_6]\cdot 3H_2O$ and $[Pb\mathbf{L2}](BPh_4)_2$. Thermodynamic parameters for protonation of ligands **L1**−**L3**. Distribution diagrams of the species for the systems **L1**/Cd(II), **L2**/Cd, and **L3**/Cd(II). UV spectra of **L3** and its Cd(II) complexes at different pH values. This material is available free of charge via the Internet at http://pubs.acs.org.

IC010597Z

---

(43) Vacca, A.; University of Florence, Florence, 1997.